

HIGH ANGLE OF ATTACK FLIGHT CONTROL OF A TAIL-SITTER UNMANNED AIRCRAFT

Daisuke Kubo*, Shinji Suzuki**

*Japan Aerospace Exploration Agency, **The University of Tokyo

Kubo.daisuke@jaxa.jp; tshinji@mail.ecc.u-tokyo.ac.jp

Keywords: *Vertical Takeoff and Landing (VTOL), Unmanned Aircraft System (UAS), Tail-Sitter, Flight Tests, Particle Image Velocimetry (PIV)*

Abstract

A prototype for a tail-sitter mini unmanned aircraft was developed, and its flight characteristics were explored in wind tunnel tests and flight tests. A tail-sitter is an aircraft that takes off and lands on its tail section with its fuselage pointing upward. A key feature of the prototype is that its wing is equipped with leading-edge slats. In previous studies, we conducted automatic high angle of attack flight tests. However, the pitch control power was found to have a poor margin. In order to achieve an improvement in the pitch control power, flow visualization was carried out via the particle image velocimetry method. The improvement in the control system was evaluated on the basis of the measured airflow data.

1 Introduction

We previously proposed a new design for a tail-sitter mini unmanned aircraft (UA) [1]. Mini UA are small, portable UA that have widespread applications in various fields, such as environmental observation, law enforcement, and disaster mitigation [2–4]. However, despite their promise, the operation of mini UA is plagued with a number of problems. One is the takeoff and landing space requirements. Although mini UA do not require runways and can be operated from a relatively small space, finding such spaces in practice is still difficult.

The landing performance of mini UA is commonly improved by using parachutes [2] and adopting the deep-stall descent technique

[5]. However, these approaches also have the disadvantages of low accuracy in arriving at the recovery point and impact shock at touchdown. Another mechanism for improving the takeoff and landing performance is a vertical takeoff and landing (VTOL) design. One of the simplest VTOL mechanisms is the tail-sitter. A tail-sitter takes off and lands on its tail section with its fuselage pointing upward. Tail-sitters have the advantage of eliminating the need for variable mechanisms to transition between hovering and cruising; therefore, this configuration is particularly suitable for mini UA with strict weight constraints because of their small size.

In previous research [1], analyses of a tail-sitter mini UA's flight characteristics using a mathematical model led to an important finding that leading-edge slats improve the descent performance during low-speed, high angle of attack (AoA) transitional flight. In order to experimentally demonstrate the effect of slats, we developed a prototype for a tail-sitter mini UA, called SkyEyeV, and verified its basic aerodynamic characteristics via wind tunnel tests [6-7]. In brief, we observed the airflow over the main wing at high AoA in a wind tunnel by the tuft method and verified the effect of the slats. We also conducted automatic high AoA flight tests. However, the pitch control power was found to have a poor margin [7]. In order to achieve an improvement in the pitch control power, we carried out flow visualization via particle image velocimetry (PIV). This paper discusses the improvement in the control system on the basis of the visualized airflows.

2 Tail-Sitter Mini UA

2.1 Concept of Design

We previously proposed a new design for a small tail-sitter UA [3]. A tail-sitter is an aircraft that takes off and lands on its tail section with the fuselage pointing upward.

A key feature of a small tail-sitter is that its wing is equipped with leading-edge slats. The propeller slipstream effect is considered to be inefficient at avoiding stall within a certain low-air-speed region [3]. This poses a grave problem for small tail-sitter UA because they have relatively low wing loading and fly at relatively low speeds. To solve this problem, we equipped the proposed UA with leading-edge slats, whose effectiveness was experimentally tested in a wind tunnel in the previous study [4,5].

2.2 Operational Scenario

Figure 1 shows the assumed operational scenario. During takeoff, the vehicle is launched by hand or by support equipment. It then climbs vertically to a certain altitude, after which it increases its flight speed and switches to forward wing-borne flight; this is called outbound transition. After completing its mission, the vehicle approaches a designated landing point. It reduces the flight speed and switches to the hovering mode; this is called inbound transition. During the final landing phase, the vehicle descends vertically and touches down on its tail landing gear; it then drops forward to touch down on its main landing gear and finally comes to rest on both the tail and main landing gears.

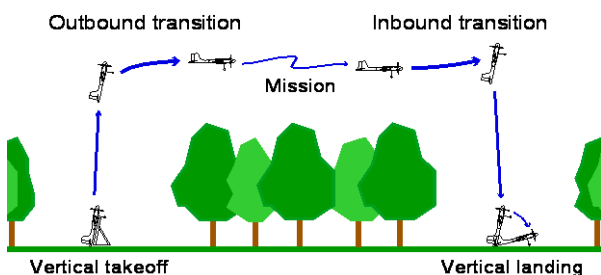


Fig. 1 Operational scenario of tail-sitter mini UA over forest area in VTOL operation

2.3 Prototype: SkyEyeV

A prototype called SkyEyeV (Fig. 2) was developed [6]. This aircraft is powered by two electric motors; it has a wingspan of 1.05 m and weighs 2.6 kg. The aircraft uses the propeller slipstream effect to avoid stall during high AoA flight (i.e., during the transition between cruising and hovering) and for attitude control during low-speed flight. The wing is equipped with semi-fixed leading-edge slats, which are manually set to the retracted or extended positions before takeoff.

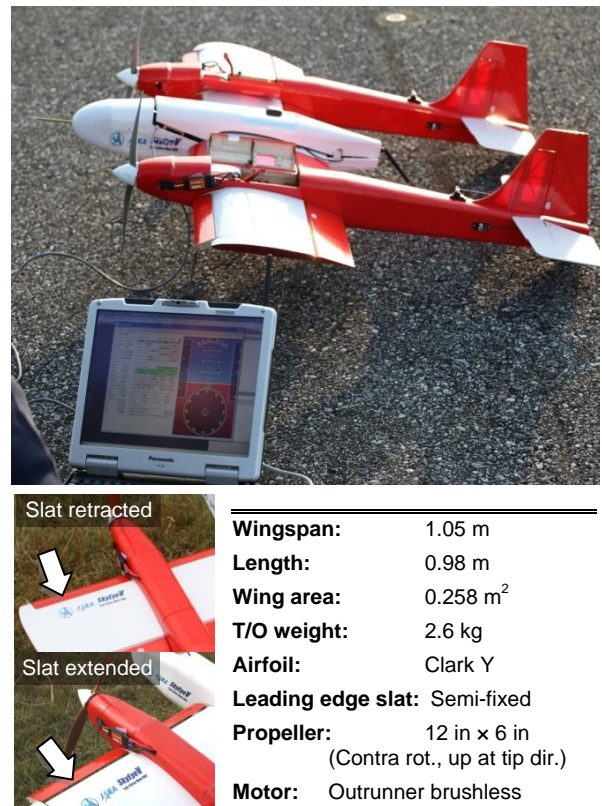


Fig. 2 Prototype of tail-sitter mini UA: SkyEyeV

3 High AoA Flight Tests

3.1 Experimental Settings

High AoA flight tests were performed to evaluate the vehicle's flight characteristics during actual flight. An autopilot system was installed in the vehicle for the flight tests. The system was specially designed for mini UA [7].

It is based on a small commercial GPS/INS for which the attitude estimation is based on quaternions and has no singularity. This feature is appropriate for tail-sitters because of their wide range of attitudes during flight (from cruising to hovering: $\theta \approx 0^\circ\text{--}90^\circ$).

3.2 Flight Tests and Results

Automatic flight tests on high AoA flight with pitch angles of up to 60° were conducted. The vehicle took off horizontally via manual control by the remote pilot. After the vehicle climbed to the cruising altitude and turned to the windward direction, which was set as the target direction in yaw control, the control mode was switched from manual to fully automatic by the remote pilot. After automatic straight flight for approximately 20 s, the control mode was switched back to manual mode. This flight pattern was repeated for each target pitch angle θ_{tar} in increments of 10° . Fig. 3 shows the test results.

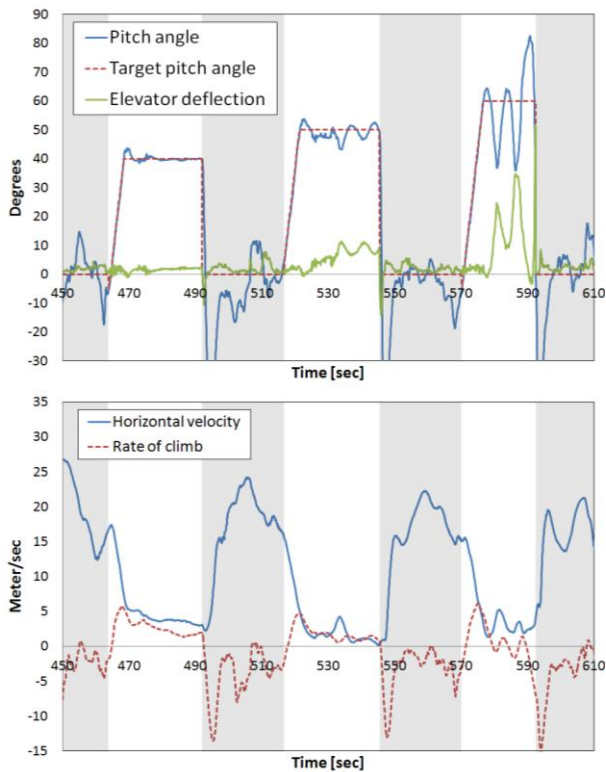


Fig. 3 High angle of attack flight test data histories (leading edge slats retracted, propeller rotation speed 6250 rpm)

At the target pitch angle θ_{tar} of 40° , the pitch angle responses were stable, and the tracking errors were sufficiently low. At θ_{tar} of 50° , the pitch angle responses fluctuated. The vehicle was able to pitch up to θ_{tar} of 60° initially, but the pitch angle responses fluctuated considerably and finally diverged. This was caused by (1) poor controllability for the elevator in high AoA flight and (2) ineffective controller design.

Problem (1) should be addressed from the viewpoint of aerodynamic design; therefore, the details of the flow field around the elevator should be investigated.

4 Flow Visualization around the Elevators

Wind tunnel tests were conducted in order to visualize and understand the flow fields around the elevators of SkyEyeV. The tests were conducted in JAXA's 2 m \times 2 m low-speed wind tunnel: a closed circuit tunnel having a 2 m \times 2 m cross section and a 4 m long test section.

4.1 PIV Experimental Settings

A two-dimensional PIV system was used in this experiment (Fig. 4).

4.1.1 PIV settings

A double-pulsed Nd:YAG laser (Quantel Twins BSL200, 200 mJ/pulse at 10 Hz) was used as the light source. The repetition rate was 4 Hz during measurement. A laser sheet was produced using a cylindrical lens. The focal length of the cylindrical lens was -70 mm. The interval of the successive laser pulse (Δt) was set at 30–40 μs depending on the wind tunnel airspeed of each test case. The laser system was mounted on the ceiling of the wind tunnel test section.

A PIV camera (LaVision, Imager Pro Plus 4M (2048 \times 2048 pixels, 14 bit)) with a lens (Nikkor 85 mm F1.4S, Nikon) was used to record the scattering light from the tracer particles; this was mounted on a traverse rail mounted on the outside wall of the test section. Two hundred pairs of pictures were taken for all

cases. The camera and laser systems were controlled using a signal generator and Lavision Davis Ver. 7.2. The analyzing software Davis 7.2 was used to calculate the velocity vectors.

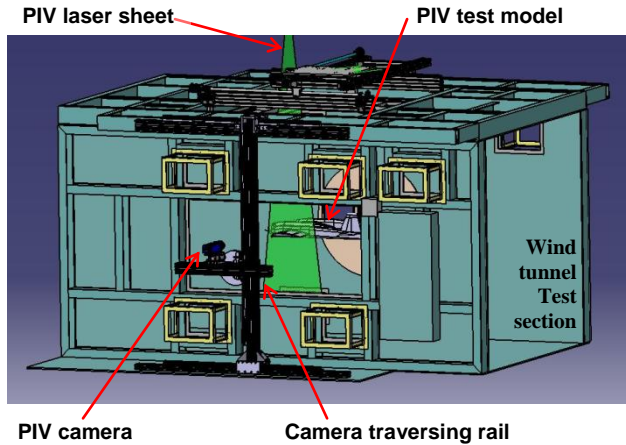


Fig. 4 PIV experimental settings on the wind tunnel test section

4.1.2 PIV test model and settings

A full-scaled SkyEyeV wind tunnel test model coated with black-colored urethane paint was used (Fig. 5). The model had shortened twin boom; it lacked tail wings to be able to avoid obstruction of the laser sheet by horizontal wings and interference of the vertical wings with the sight line of the PIV camera. The propellers were driven by power supplied from batteries installed in the fuselage, and the rotational speed of the propeller was maintained at 6500 rpm using a wireless remote. The model was supported by a robotic arm in the test section. The attaching rod had an AoA offset pivot with increments of 30° : 0° , $+30^\circ$, and $+60^\circ$. Since the sting arm traveled from -10° to $+30^\circ$, the AoA of the vehicle could be set anywhere between -10° and $+90^\circ$.

The position of the cross section of the laser sheet was located at the center of the inboard part of the left wing (Fig. 6). Since the traversing range of the laser system was limited, the model was adjusted to the desired position using arm movement of the supporting robotic arm.

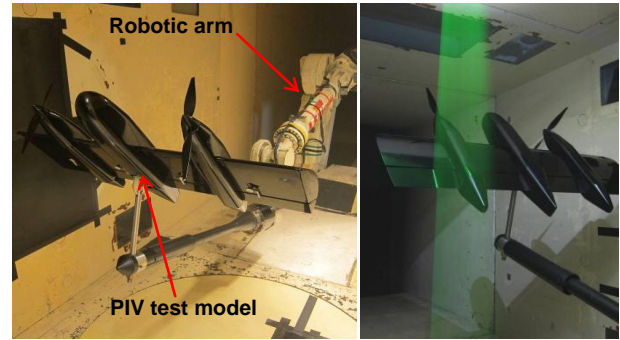


Fig. 5 PIV test model and settings on the robotic arm in the wind tunnel test section (left) and laser sheet at the elevator position (right)

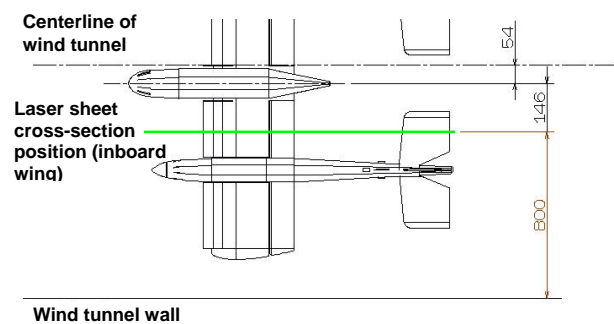


Fig. 6 Horizontal position of the laser sheet cross section (tail wings are illustrated only for reference)

4.2 Results

The averaged velocity vectors were calculated from the recorded 200 pairs of pictures, and the airflow fields were visualized. The results are illustrated in Figs. 7–12. The absolute values of the velocity vectors (m/s) are shown using colored contours. The tail wings are illustrated only for reference of the position; the experiment was performed without the tail parts (see section 4.1.2).

4.2.1 $AoA = 30^\circ$

The visualized flows around the elevator positions are illustrated in Figs. 7 and 8 for airspeeds of 5.4 and 10.8 m/s, respectively.

Although the major part of the slipstreams (flow speed of about 20 m/s) hit the elevator position at airspeed of 5.4 m/s, the slipstream did not hit the elevator position at the 10.8 m/s airspeed. However, this was not a serious problem, because the dynamic pressure of the non-core flow (nearly equal free stream of the

wind tunnel) was sufficiently high and the moment arm of the pitch control was long. No problems occurred for the $AoA = 30^\circ$ flights.

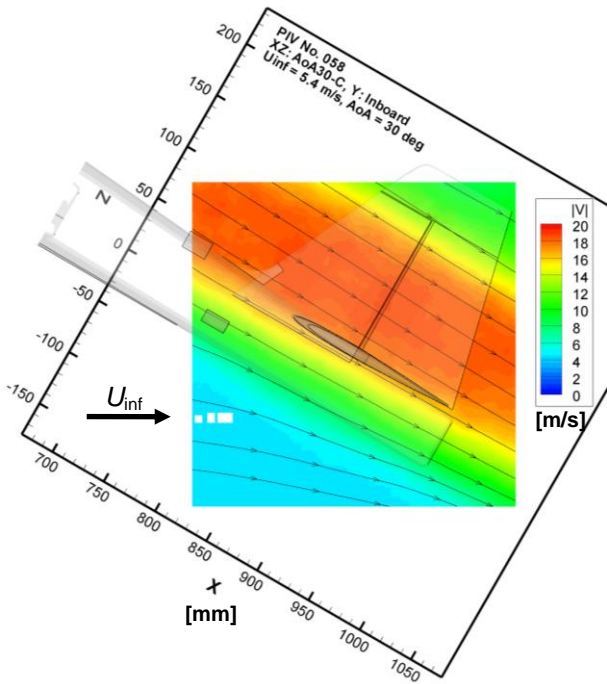


Fig. 7 PIV image of airflow field at the elevator position with $AoA = 30^\circ$ and $U_{inf} = 5.4$ m/s

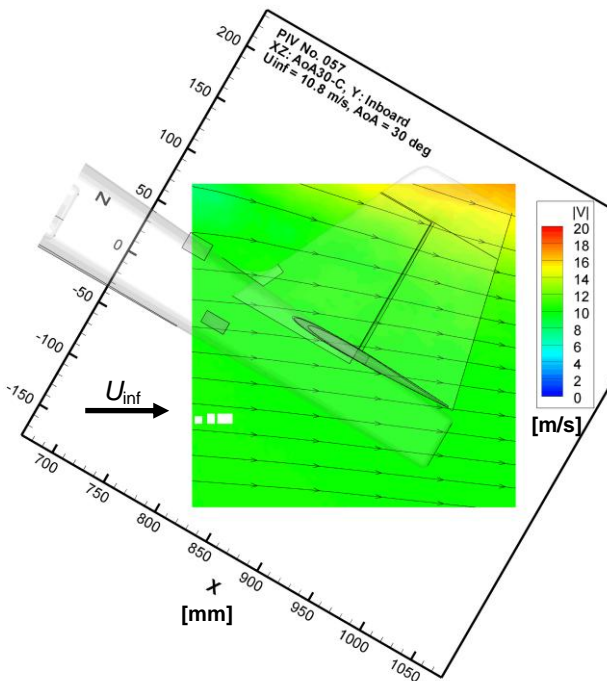


Fig. 8 PIV image of airflow field at the elevator position with $AoA = 30^\circ$ and $U_{inf} = 10.8$ m/s

4.2.2 $AoA = 45^\circ$

The visualized flows are illustrated in Figs. 9 and 10 for airspeeds of 3.0 and 5.0 m/s, respectively. Although the major part of the slipstreams (flow speed from 10 to 14 m/s) hit the elevator position for the 3.0 m/s case (Fig. 9), the slipstream rarely hit the elevator position for the 5.0 m/s case (Fig. 10). Even for the 5.0 m/s case, this was still not a serious problem, because the dynamic pressure of the flow around the elevator position was sufficient and the moment arm of the pitch control was not short. No problem occurred for the $AoA = 45^\circ$ flights as well.

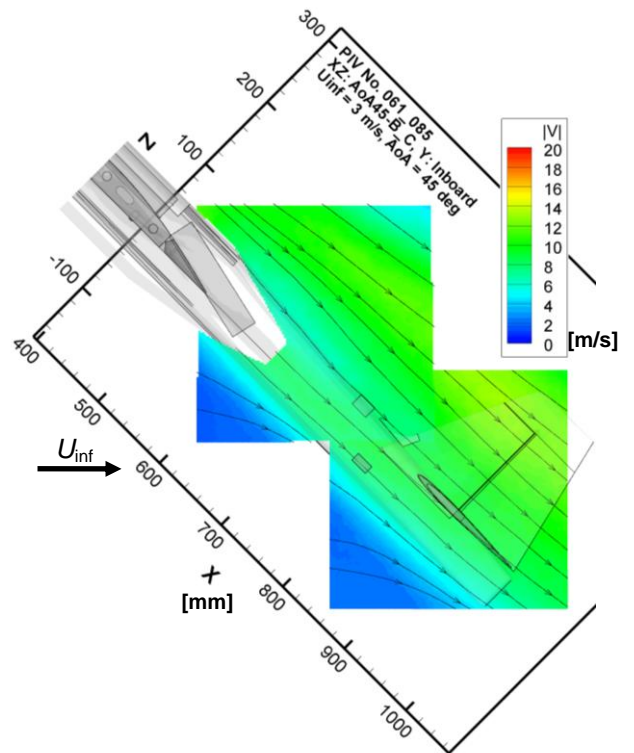


Fig. 9 PIV image of airflow field at the elevator position with $AoA = 45^\circ$ and $U_{inf} = 3.0$ m/s

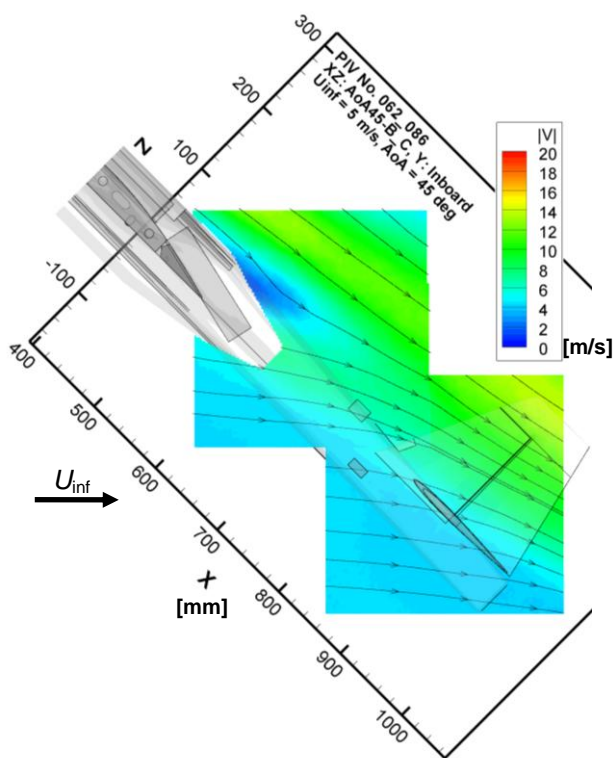


Fig. 10 PIV image of airflow field at the elevator position with $AoA = 45^\circ$ and $U_{inf} = 5.0$ m/s

4.2.2 $AoA = 60^\circ$

The visualized flows are illustrated in Figs. 11 and 12 for airspeeds of 2.5 and 5.0 m/s, respectively. Even for the 2.5 m/s case (Fig. 11), the slipstream did not hit the elevator position. This is a serious problem because the dynamic pressure of the flow around the elevator position was not sufficiently high and the moment arm of the pitch control was very short. This shows that the elevator effectiveness is strongly affected by the flight speed (or gusts), which is a serious problem during high AoA flights. The poor margin of the pitch control power that was indicated in the high AoA flight tests was caused by this mechanism.

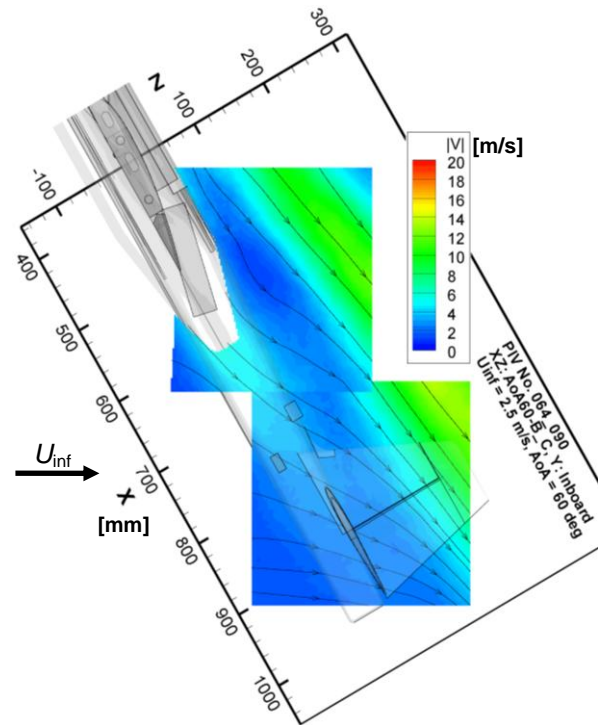


Fig. 11 PIV image of airflow field at the elevator position with $AoA = 60^\circ$ and $U_{inf} = 2.5$ m/s

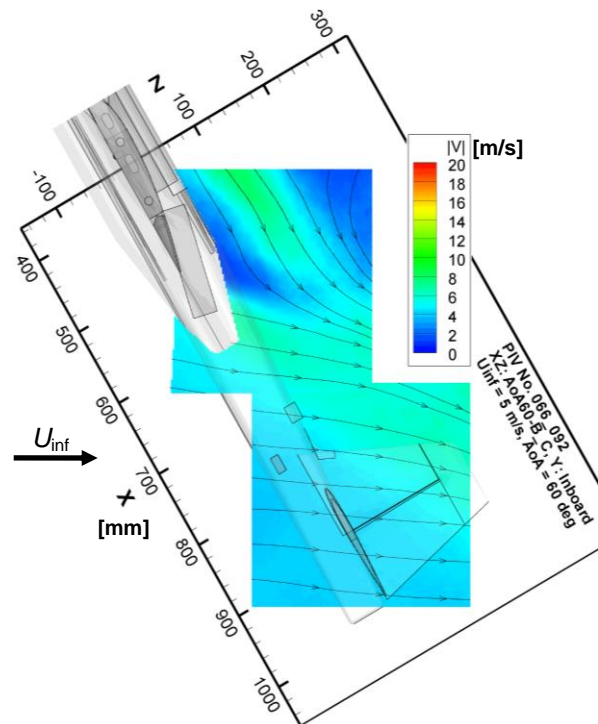


Fig. 12 PIV image of the airflow field at the elevator position with $AoA = 60^\circ$ and $U_{inf} = 5.0$ m/s

5 Improvement in Pitch Control Power

The results of the automatic high AoA flight test and the visualized airflow data indicated that the

propeller-slipstream-immersed elevator concept for pitch control of a tail-sitter aircraft is inadequate. Another mechanism for pitch control should be adopted.

One option is the introduction of a cyclic pitch control mechanism into the twin propellers—i.e., *rotors* like helicopters. The collective variable blade-pitch capability of rotors also provides the advantage of greatly improving the tail-sitter aircraft's flight efficiency because it can be optimized for both the hovering mode and the cruising mode. However, the biggest disadvantage of the rotor approach is the increased mechanism complexity and weight of the aircraft.

Another option is to adopt a variable blade-pitch propeller system (with an outrunner brushless motor) [8] equipped with the rear part of the aircraft pointed in the Z direction for the aircraft's pitch control (Fig. 13). Although the system can only be used for pitch control purposes, commercial-off-the-shelf parts can be easily acquired from radio-control model airplane markets.

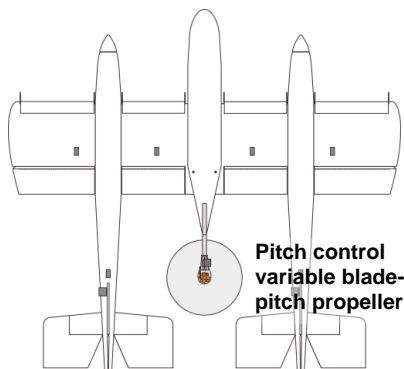


Fig. 13 An approach to improve the pitch control power of SkyEyeV

6 Conclusions and Future Work

A prototype for a tail-sitter mini unmanned aircraft (UA), called SkyEyeV, was developed, and automatic high angle of attack (AoA) flight tests and airflow visualizations were conducted via particle image velocimetry (PIV). The high AoA flight tests revealed a poor margin of the pitch control power; this was confirmed from the visualized airflow data around the elevator position of the tail-sitter. This is a serious problem for the design concept. However,

several options are available for improving the pitch control power.

Autonomous high AoA flight tests including the available options will be demonstrated in the near future.

References

- [1] Kubo D and Suzuki S. Tail-Sitter Vertical Takeoff and Landing Unmanned Aerial Vehicle: Transitional Flight Analysis, *Journal of Aircraft*, Vol. 45, No. 1, pp. 292–297, 2008.
- [2] Hirokawa R, Kubo D, Suzuki S, Meguro J, and Suzuki T. A Small UAV for Immediate Hazard Map Generation, *Proceedings of Infotech@Aerospace 2007*, Rohnert Park, California, AIAA Paper 2007-2725, 2007.
- [3] Abershitz A, Penn D, Levy A, Shapira A, Shavit Z, and Tsach S. IAI's Micro/Mini UAV Systems-Development Approach, *Proceedings of Infotech@Aerospace 2005*, Arlington, VA, AIAA Paper 2005-7034, 2005.
- [4] Schulz H W, Buschmann M, Kordes T, Kruger L, Winkler S, and Vorsmann P. The Autonomous Micro and Mini UAVs of the CAROLO-Family, *Proceedings of Infotech@Aerospace 2005*, Arlington, Virginia, AIAA 2005-7092, 2005.
- [5] Taniguchi H. Analysis of Deepstall Landing for UAV, *Proceedings of ICAS2008*, ICAS 2008-5.6.4, 2008.
- [6] Kubo D, Muraoka K, Okada N, Naruoka M, Tsuchiya T, and Suzuki S. Flight Tests of a Wing-in-Propeller-Slipstream Mini Unmanned Aerial Vehicle, *Proceedings of AIAA Unmanned...Unlimited Conference*, Seattle, Washington, AIAA-2009-2070, 2009.
- [7] Kubo D, Muraoka K, and Okada N. High Angle of Attack Flight Characteristics of a Wing-in-Propeller-Slipstream Aircraft, *Proceedings of ICAS2010*, ICAS2010-6.8.3, 2010.
- [8] EVP unit: <http://www.modelmotors.cz/> (cited on 1st June 2012)

Copyright Statement

The authors confirm that they, and/or their company or organization, hold copyright on all of the original material included in this paper. The authors also confirm that they have obtained permission, from the copyright holder of any third party material included in this paper, to publish it as part of their paper. The authors confirm that they give permission, or have obtained permission from the copyright holder of this paper, for the publication and distribution of this paper as part of the ICAS2012 proceedings or as individual off-prints from the proceedings.